

RESEARCH ARTICLE

Interrogation of phosphor-specific interaction on a high-throughput label-free optical biosensor system—Epic[®] system

Meng Wu¹, Shunyou Long¹, Anthony G. Frutos², Maryna Eichelberger³, Min Li¹, and Ye Fang²

¹Department of Neuroscience, High Throughput Biology Center and Johns Hopkins Ion Channel Center (JHICC), Johns Hopkins University, School of Medicine, Baltimore, Maryland, USA, ²Corning Incorporated, Science and Technology Division, Corning, New York, USA, and ³Center for Biologics Evaluation and Research, Food and Drug Administration, Bethesda, MD, 20892, USA

Abstract

The Epic[®] system, a high-throughput label-free optical biosensor system, is applied for the biochemical interrogation of phosphor-specific interactions of the 14-3-3 protein and its substrates. It has shown the capability not only for high-throughput characterization of binding rank and affinity but also for the exploration of potential interacting kinases for the substrates. A perspective of biochemical applications for diagnostics and biomarker discovery, as well as cell-based applications for endogenous receptors and viral infection characterization, are also provided.

Keywords: Label free; phosphor-specific; Epic[®]; 14-3-3; kinase

Introduction

Label-free detection technologies have been widely used to characterize biomolecular interactions without having to label the target molecules (1,2). Different transduction techniques, such as surface plasmon resonance (SPR), optical ellipsometry, quartz crystal microbalance, Raman scattering, and calorimetry, have been developed. Despite their diverse applications, most of their compatibility with high-throughput screening remains a challenge, although recent developments [i.e., SPR imaging (3), or incidence-angle dependence of optical reflectivity difference imaging (4)] have shown the potential for increasing throughput. Currently, resonant waveguide grating (RWG) sensors have been developed into a high-throughput microplate-based biosensor—the Epic[®] system—combining the features of label-free detection with high-throughput capability (5). Label-free optical biosensors offer the possibility to develop a generic assay for evaluating protein–protein interactions specific to phosphorylated target sequences (6).

Phosphorylation is a key posttranslational process that confers diverse regulation in biological systems involving specific protein–protein interactions recognizing the phosphorylated motifs (7). Of great interest for ion channels, which represent an important but underdeveloped class of drug targets, is the surface expression of these membrane proteins modulated by the posttranslational phosphorylation. A common effect of phosphorylation is a change in protein–protein interactions. 14-3-3s were the first protein modules to be identified as binding specifically to phosphorylated substrates (8,9). Evidence from structural studies and sequence analyses indicates that the primary function of 14-3-3 proteins lies in their preferential binding to phosphorylated substrates, through their antiparallel bivalent binding sites. In addition to known canonical binding motifs, several earlier reports have identified interactions between 14-3-3 proteins and the C-termini of target proteins. This characteristic binding (i.e., SWpTY motif, proposed as Mode III) (10), has high-binding affinity that is comparable to that of the canonical binding motifs (11).

Address for Correspondence: Min Li, Ph.D., Department of Neuroscience, High Throughput Biology Center and Johns Hopkins Ion Channel Center (JHICC), Johns Hopkins University, School of Medicine, 733 North Broadway, BRB311, Baltimore, MD 21205. E-mail: minli@jhmi.edu

Recently, studies have suggested that 14-3-3 proteins, through binding to inducible phosphorylated motifs, regulate protein expression on the cell surface (9).

Currently, multiple methods are available for detecting phosphorylation (12), including antibodies-based fluorescent detection, radioactive-ATP, and fluorescent-labeled peptide substrates for FRET (13), or fluorescence polarization detection (14). Although above mentioned methods have offered a wide range of choices for characterization of phosphorylation, and potentially for the development of high-throughput screening assays, these label-based methods are prone to artifacts and other detrimental effects [i.e., label effect on antibody interactions (15)]. Here we present our results from use of a high-throughput label-free optical biosensor system—Epic®—for the interrogation of phosphor-specific interaction of 14-3-3 with SWpTY motif.

Label-free characterization of 14-3-3 AND SWpTY peptide

Assay principle of biosensors

The Epic® system is based on a resonant waveguide grating (RWG) biosensor, which exploits the evanescent wave that is generated by the resonant coupling of light into a waveguide via a diffraction grating. The guided light can be viewed as one or more mode(s) of light that all have directions of propagation parallel with the waveguide, due to the confinement by total internal reflection at the substrate-film and medium-film interfaces. The waveguide has a higher refractive index value than its surrounding media. Because the guided light mode has a transversal amplitude profile that covers all layers, the effective refractive index N of each mode is a weighted sum of the refractive indices of all layers:

$$N = f_N(n_F, n_S, n_C, n_{ad}, d_F, d_{ad}, \lambda, m, \sigma) \quad (1)$$

Here, n_F , n_S , n_C , and n_{ad} is a refractive index of the waveguide, the substrate, the cover medium, and the protein adlayer, respectively; d_F and d_{ad} are the effective thickness of the film and of the protein adlayer, respectively. λ is the vacuum wavelength of the light used. $m=0, 1, 2$, is the mode number; and σ is the mode type number, which equals to 1 for TE (transverse electric or s -polarized) and 0 for TM modes (transverse magnetic or p -polarized). Because of its higher sensitivity, generally the TM_0 was used for measuring the binding of biomolecules to the probe proteins immobilized on the surface of the waveguide substrate.

When a laser illuminates the waveguide at varying angles or wavelengths, light is coupled into the waveguide only at specific angles or wavelengths, respectively. This coupling is determined by the effective refractive index

of the guided mode, denoted as N . The value of N can be calculated numerically from the mode equation for a given mode of a four-layer waveguide configuration (16,17).

$$0 \cong \pi m - k(n_F^2 - N^2)^{0.5} + \arctan \left[\frac{d_F + d_A \frac{n_A^2 - n_C^2}{n_F^2 - n_C^2} \left[\frac{(N/n_C)^2 + (N/n_A)^2 - 1}{(N/n_C)^2 + (N/n_F)^2 - 1} \right]^\sigma}{\left(\frac{n_F}{n_S} \right)^2 \left(\frac{N^2 - n_S^2}{n_F^2 - N^2} \right)^{0.5}} \right] + \arctan \left[\frac{\left(\frac{n_F}{n_C} \right)^2 \left(\frac{N^2 - n_C^2}{n_F^2 - N^2} \right)^{0.5}}{\left(\frac{n_F}{n_C} \right)^2 \left(\frac{N^2 - n_C^2}{n_F^2 - N^2} \right)^{0.5}} \right] \quad (2)$$

Here, $k=2\pi/\lambda$.

Since the laser light is coupled to, and propagates parallel to the surface in the plane of a waveguide film, this creates an electromagnetic field (i.e., an evanescent wave) in the liquid adjacent to the interface. The amplitude (E_m) of the evanescent wave decays exponentially with increasing distance d from the interface:

$$E_m(d) = E_m(0) \exp\left(\frac{-d}{\Delta Z_C}\right) \quad (3)$$

with:

$$\Delta Z_C = \frac{1 - \sigma}{k(N^2 - n_C^2)^{0.5}} + \frac{\sigma \left[(N/n_F)^2 + (N/n_C)^2 - 1 \right]^{-1}}{k(N^2 - n_C^2)^{0.5}} \quad (4)$$

Where “Delta”Zc is the penetration depth (also termed as sensing volume; typically ~150 nm) of the evanescent tail of the waveguide mode that extends into the cover medium. This means that a target or complex of a certain mass contributes more to the overall response when the target or complex is closer to the sensor surface, compared to when it is further from the sensor surface.

Figure 1 showed a schematic drawing for detecting the binding of biomolecules in a sample to the probe molecules immobilized onto the surface of the waveguide substrate. In a particular assay, the probe molecules are precoupled to the surface, primarily through covalent-coupling or biospecific interaction (e.g., biotin-avidin interaction). Alternatively, the immobilization of probe molecules can be monitored in real time to ensure the efficiency and quality of the coupling. Nonetheless, after the immobilization of probe molecules, the binding of target molecules, in the absence and presence of a modulator, can be directly monitored by the label-free RWG biosensor, as manifested by the shift in wavelengths or angles of the reflected light.

The Corning Epic® system is composed of three major components for bioassay applications: an EPIC® sensor microplate, an RWG detector, and a liquid-handling system. The sensor microplate consists of a glass bottom plate attached to a holey plastic 384-well plate, which enables high-throughput screening. The RWG sensor consists of a thin film of dielectric material on the grating presenting glass substrate.

Principle of biochemical assays

The label-free detection of 14-3-3 interactions with its phosphorylated partners was performed by using a resonant waveguide grating system known as the Epic® system. The detection scheme is based on the direct covalent immobilization of NH₂-SWpTY (NH₂AhxAhxFRGRSWpTY-COOH) peptide on the surface of the Epic® plates (Figure. 2A). SWpTY is a member of the mode III consensus motif family that interacts with 14-3-3 (10). In solution, synthetic SWpTY peptide binds to recombinant 14-3-3 with a dissociation constant (K_D) of 0.17 μ M, comparable to the affinity of canonical modes I and II binding (11). The Epic® system exploits the evanescent wave that is generated by the resonant coupling of light into a waveguide via a diffraction grating (16). Hence, the interactions within ~150 nm vertical range may be detected with no requirement for removal of the interaction solution. Furthermore, the microtiter plate format of the Epic® system allows for the open access to parallel and sequential additions of analytes, a feature that is more difficult to implement in a flow cell-based system.

Figure 2B shows, upon GST-14-3-3 ζ addition, the sample well with bound GST-14-3-3 ζ on the NH₂-SWpTY-immobilized surface gives a binding signal, while the unbound 14-3-3 out of the ~150 nm penetration depth is not detected. Conversely, the reference well with a PEG-amine immobilized surface gives very low signal upon GST-14-3-3 ζ addition.

Figure 2C shows the evolution of the binding signal as a function of time. Unlike SPR experiments performed with flow channels, in which true kinetic measurements can be made, the binding in the Epic® plates is diffusion limited, and, therefore, *kinetic* measurements are also diffusion limited. Nonetheless, equilibrium-binding measurements and estimation of affinity can be accurately determined.

K_d detection with Epic®

To determine the rank order of the affinity of various peptides for 14-3-3, a competition assay was conducted. In contrast to the direct detection using the immobilized binding partner, the competition assay uses the binding competitors to measure binding

affinity in solution. Affinity detection through competitive replacement has been a routine method (18,19). The distinct signals by competitor peptides can be observed with considerably different affinities using the Epic® system. The fitting results for K_D values of the competitors SWpTY, SWTY, SWpTD, and SWpTP are $0.12 \pm 0.05 \mu$ M, $> 50 \mu$ M, $1.75 \pm 0.14 \mu$ M, and $6 \pm 1.67 \mu$ M, respectively. Direct comparison of this method with the previous detection of SWTY-14-3-3 interaction with fluorescence anisotropy suggests a similar rank order of the affinity.

Assay sensitivity and specificity

Using the optimized conditions for GST-14-3-3 ζ , the assay has a limit of detection of 38 nM, with a linear range (LR) of 0.038–2 μ M ($R^2=0.96$). To evaluate the specificity of the interaction, 14-3-3 was added into wells modified with either NH₂-SWpTY or nonphosphorylated NH₂-SWTY (Fig. 3A). Only wells immobilized with the phosphorylated peptide NH₂-SWpTY gave detectable signals. Furthermore, upon addition of competitive 14-3-3 binding peptides, SWpTY, or R18, a nonhomologous 14-3-3 binding peptide, the binding signals were significantly reduced. In contrast, the nonphosphorylated SWTY peptide did not affect the binding of 14-3-3. To be more definitive, the SWpTY peptide binding was tested with wild-type 14-3-3 and 14-3-3 K49E, which has a mutation at the binding site (20). Consistently, the binding signal was obtained only in wild-type 14-3-3 proteins. Therefore, these experimental results provide the evidence for the specific phosphor-dependent detection of 14-3-3 interactions with substrate peptides.

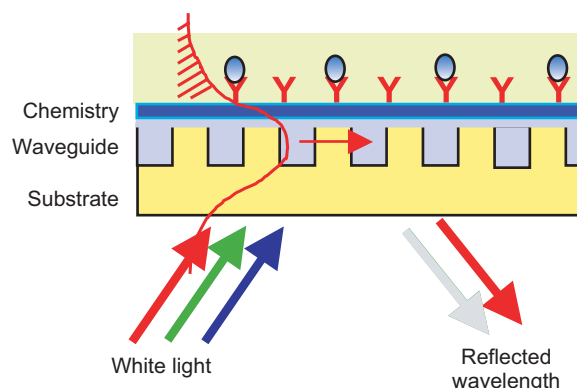


Figure 1. The detection scheme of RWG biosensor for detecting the binding of target molecules (●) in a sample to the probe molecules (Y) immobilized onto the surface of a waveguide substrate. The specific binding event is manifested in a shift in the wavelength of the reflected light. The waveguide substrate consists of a region within which a grating structure is embedded. The probe molecules are coupled to the derivatized waveguide substrate.

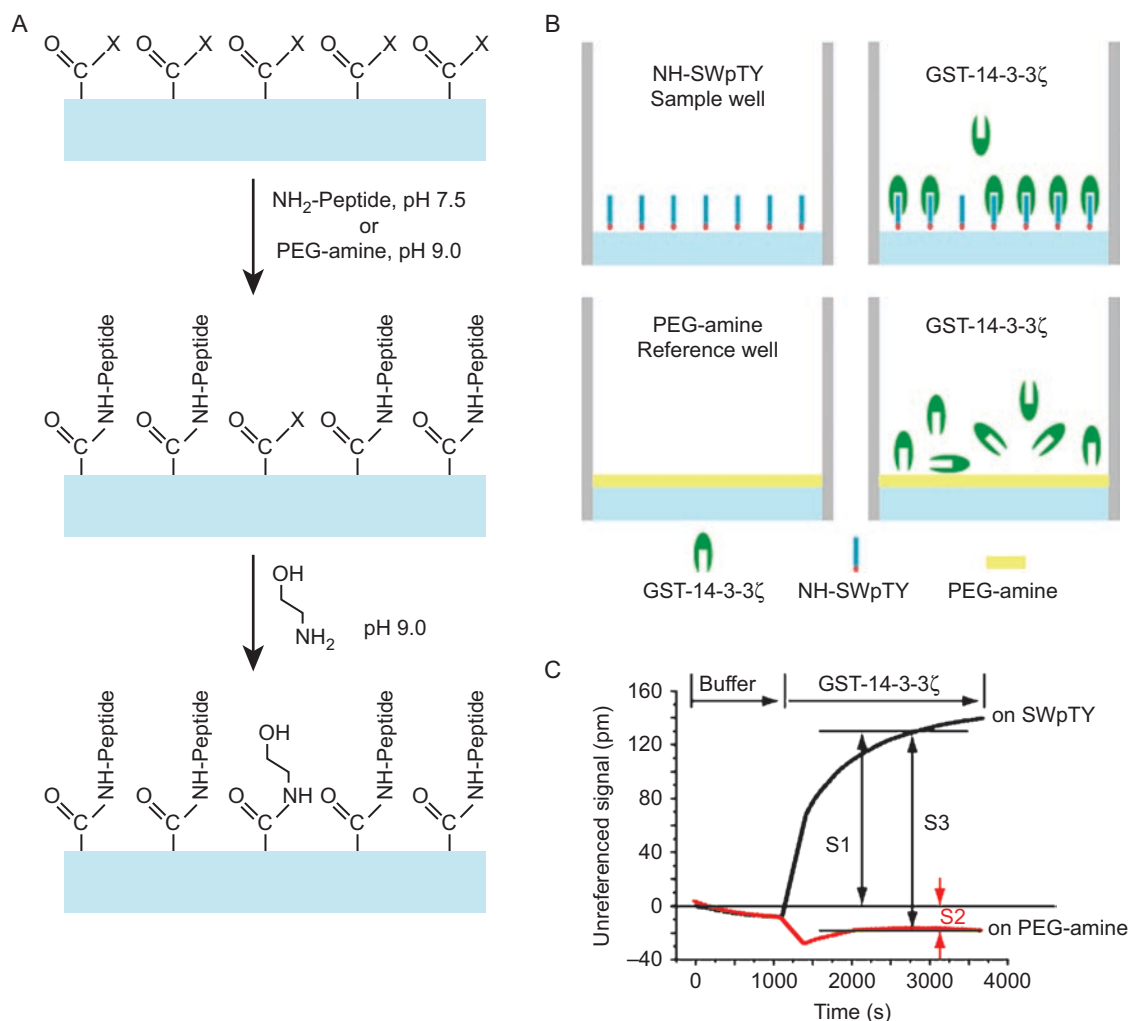


Figure 2. Scheme of 14-3-3 SWpTY interaction detection. (A) Surface reaction scheme for immobilization of N-terminal amino group modified peptides. X, reactive group; $\text{NH}_2\text{-Peptide}$, N-terminal amino group modified peptides. (B) Binding scheme for 14-3-3. Left two panels show the immobilized substrate ($\text{NH}_2\text{-SWpTY}$) and reference (PEG-amine). Right two panels show $\text{GST-14-3-3}\zeta$ binding. In the sample well, where $\text{GST-14-3-3}\zeta$ is added, $\text{GST-14-3-3}\zeta$ binds to the immobilized $\text{NH}_2\text{-SWpTY}$ peptide. In the reference well containing immobilized PEG-amine , there is no binding of $\text{GST-14-3-3}\zeta$. (C) The time-course charts of the respective responses from sample wells and reference wells, with S1 as an unreferenced signal from $\text{GST-14-3-3}\zeta$ on $\text{NH}_2\text{-SWpTY}$ ($50\ \mu\text{g}/\text{mL}$ at pH 5.5, GST-14-3-3 at $1\ \mu\text{M}$), S2 as an unreferenced signal from $\text{GST-14-3-3}\zeta$ on PEG-amine ($50\ \mu\text{g}/\text{mL}$, pH 9.0, GST-14-3-3 at $1\ \mu\text{M}$), and S3 as a referenced signal obtained by subtraction of S1 with S2.

Compatibility of the Epic® system for high-throughput screening

The detection of 14-3-3 binding by the Epic® system was further examined for the capability of high-throughput screening. Common to most label-free systems is the issue of nonspecific interactions, which require control tests for the small molecules, especially those promiscuous, hydrophobic ones. To overcome this issue, a self-reference Epic® plate has been designed, as shown in Figure 3. One half of the sensor was coated with active chemical, good for immobilization; the other half was not coated and was resistant to the immobilization and consequently serves as the control. The Epic® system can detect two areas and normalize the nonspecific interaction with the surface

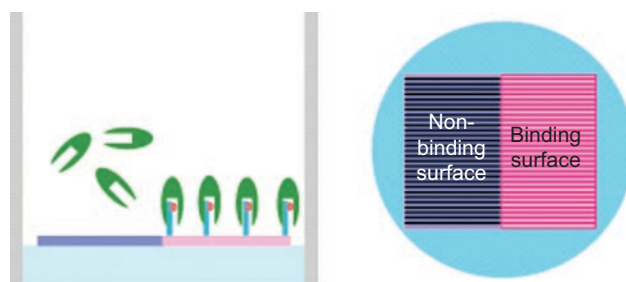


Figure 3. Schematic representation of the self-referenced biosensor in the well of Epic® plates. The pink area denotes the active chemical area good for immobilization, whereas the gray area denotes the area resistant to immobilization, which consequently serves as the control. The Epic® system can detect two distinct areas and normalize the nonspecific interaction with the surface from the promiscuous small molecules/aggregates.

from the promiscuous small molecules/aggregates. For example, as expected, the presence of DMSO did result in a change of bulk refractive index, and, hence, a change in the unreferenced signals of both test wells and reference wells. However, proper use of referencing eliminates this effect, and thus there is no significant difference for the referenced signals between 0% DMSO up to 10% DMSO.

The statistic data of responses of GST-14-3-3 ζ , with or without preincubated SWpTY, have shown a good signal-to-noise ratio of ~ 15 . The addition of 20 μM of competitor SWpTY peptide in the solution resulted in a 94% decrease of the referenced signals, with a Z factor of 0.8, indicating the robustness and compatibility of the assay for high-throughput screening.

Label-free detection of phosphorylated SWpTY peptide

Because of the specificity of the Epic[®] system for the label-free detection of the phosphor-dependent interaction of 14-3-3 and its substrate, SWpTY, a label-free assay for kinase identification of the peptide substrates is designed with two possible schemes.

The first approach (Figure. 4A) is the direct identification of acting kinases by immobilization of the nonphosphorylated peptide substrate on the optical sensor. The in situ and in vitro phosphorylation system will be added into wells to phosphorylate the immobilized peptide substrates, consequently inducing the 14-3-3 binding and biosensor signals. The second approach (Figure. 4B) is the indirect identification of acting kinases by immobilization of the phosphorylated peptide substrate on the optical sensor. The in situ and in vitro phosphorylation system will be added into wells with nonphosphorylated peptide substrate in solution, and after phosphorylation, the newly produced phosphorylated peptide substrate will compete with the immobilized peptide substrates for the 14-3-3 binding and biosensor signals. The second approach is more likely suitable for the homogeneous phosphorylation of the peptide substrate. The first approach will be limited by the accessibility of the immobilized peptide substrates. As shown in Figure 4C, both approaches were tested in a case. When a nonphosphorylated peptide is immobilized, the addition of phosphorylation mixture (rxn) does not generate any 14-3-3 binding at the second addition. This validates that 14-3-3 does not bind to nonphosphorylated peptide, and phosphorylation is not working for immobilized nonphosphorylated peptide by Akt and PKA. Conversely, when a phosphorylated peptide is immobilized, the addition of phosphorylated peptide (positive control) results in a great decrease of

the Epic[®] signal, due to the competition, while 14-3-3 alone (negative control) generates a higher binding signal. When Akt is added, the mixture results in $\sim 40\%$ decrease of the 14-3-3 binding signal (newly produced SWpTY competing with immobilized SWpTY), while the addition of PKA results in no change of the 14-3-3 binding signal. Preliminarily, the results indicate that Akt (21) is likely to be the acting kinase (at least in vitro) for SWTY, while PKA is unlikely to be the acting kinase for SWTY.

Discussion and perspectives

Comparison of characterization of 14-3-3 and SWpTY interaction by Epic[®] System with that by fluorescence anisotropy

The phosphor-specific interactions of the 14-3-3 and SWpTY are characterized by two different methods: one label method of fluorescence anisotropy, and another by the Epic[®] label-free system. As indicated in Table 1, the two methods have very similar results in sensitivity, affinity detection, and affinity ranking of SWTY-like peptides. Both have shown robustness for the high-throughput screening, with a Z factor better than 0.5, S/N ratio better than 7, and up to a 10% DMSO tolerance (with self-reference).

Perspectives

One possible immediate application is likely to be the antibody profiling for the discovery of biomarkers in the blood/serum samples. Our preliminary data with an Anti-SWpTY phosphorylation-specific antibody have shown that the antibody has better sensitivity than that of 14-3-3 (data not shown). In addition, IgG and Anti-IgG interaction can be fairly well detected on the Epic[®] label-free system, which can discriminate the difference between natural Anti-IgG and Fluorescein-labeled Anti-IgG (data not shown). These results have indicated the possibility of high-throughput profiling of the antibodies for the large-scale biomarker discovery, especially in a label-sensitive pathway-based biomarker search (22).

One great aspect of Epic[®] application is the cell-based label-free assay. There have been quite a few reports on its potential applications. One of our applications is the direct detection of endogenous receptors in A431 cells. As shown in Figure 5, a small-scale screen on Epic[®] has results in several interesting small molecules, including known modulators. Comparing with the kinetic Ca-Fura II imaging results (23), the label-free kinetics have a very similar shape of time-course response, which might indicate a delayed response correlated with Ca response. This may provide a basis for further investigation of the

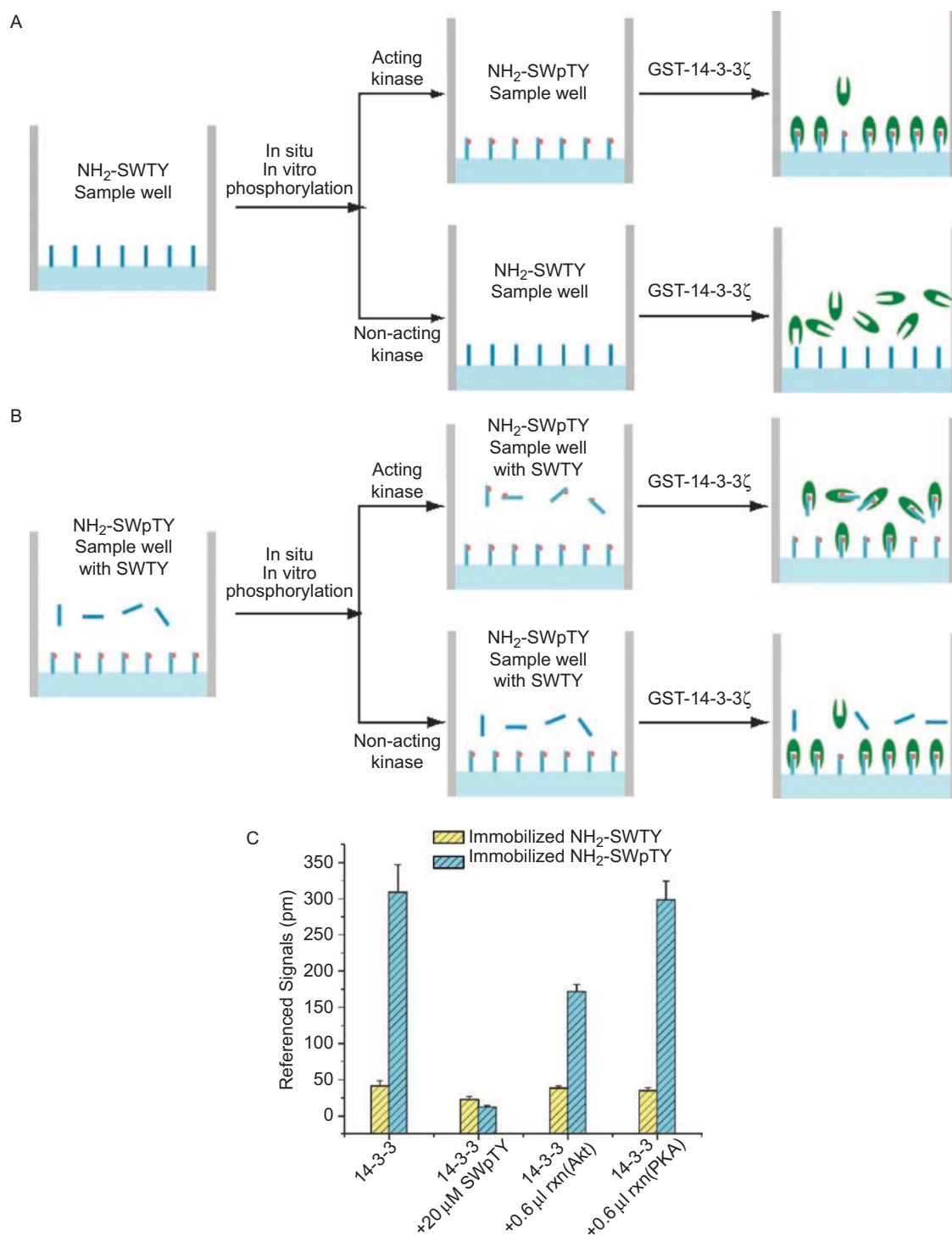
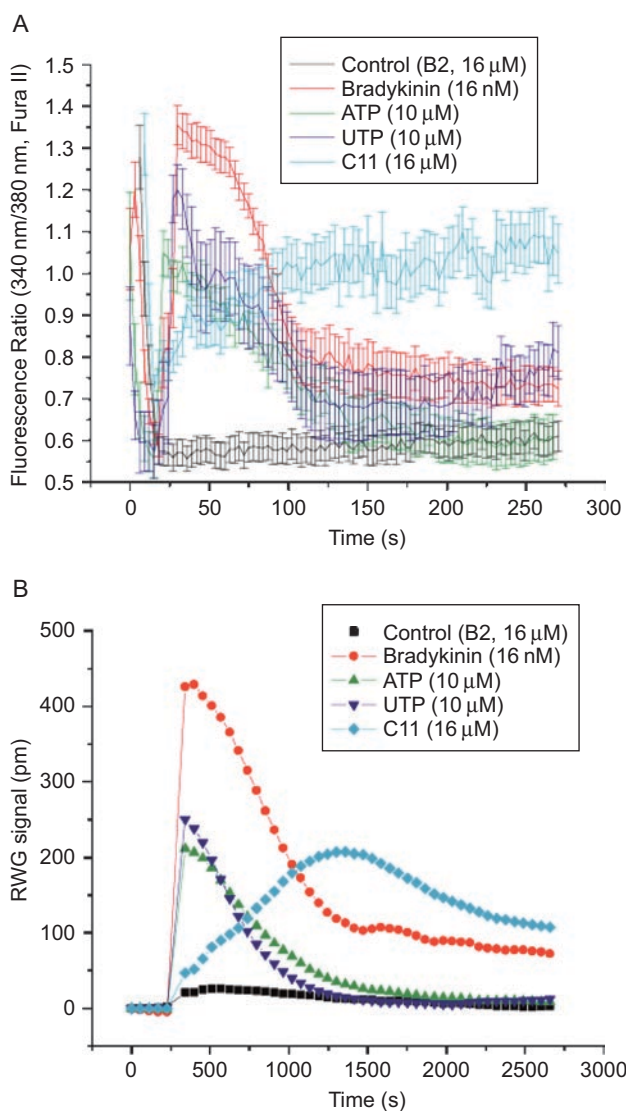


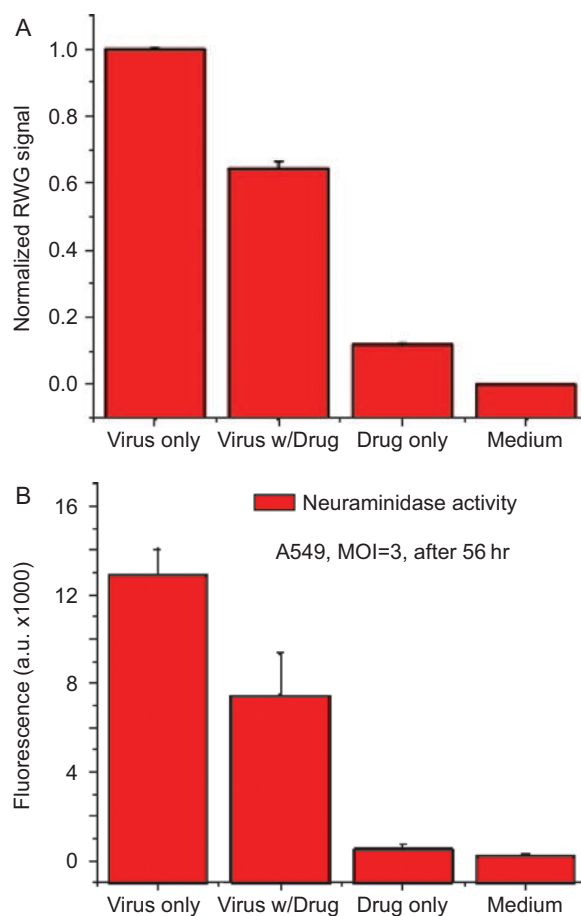
Figure 4. Schematic representation of the two approaches for kinase identification of peptide substrates, as indicated by 14-3-3 and SWTY pair. (A) Direct identification of acting kinases by immobilization of the nonphosphorylated peptide substrate on the optical sensor. The in situ and in vitro phosphorylation system will be added into wells, to phosphorylate the immobilized peptide substrates and consequently induce the 14-3-3 binding and biosensor signals. (B) Indirect identification of acting kinases by immobilization of the phosphorylated peptide substrate on the optical sensor. The in situ and in vitro phosphorylation system will be added into wells with nonphosphorylated peptide substrate in solution, and after phosphorylation, the newly produced phosphorylated peptide substrate will compete with the immobilized peptide substrates for the 14-3-3 binding and biosensor signals. (C) Epic[®] signal as for kinase identification for SWTY phosphorylation. Akt and PKA were used in the optimal condition of phosphorylation. The 20 μM SWpTY was added as a positive control.

Table 1. Comparison of the 14-3-3-SWpTY interaction detection from fluorescence anisotropy and Epic[®] label-free detection.

	Fluorescence Anisotropy				Epic [®] System			
	SWpTY	SWTY	SWpTD	SWpTP	SWpTY	SWTY	SWpTD	SWpTP
Sensitivity	16 nM				38 nM			
Linear range	16–700 nM				38–2000 nM			
Specificity	Good				Good			
Affinity (μM)	$K_D=1.7\pm 0.3$ (GST-14-3-3 ζ)				$K_D=2.1\pm 0.4$ (GST-14-3-3 ζ)			
Affinity (μM , competitive)	SWpTY	SWTY	SWpTD	SWpTP	SWpTY	SWTY	SWpTD	SWpTP
	0.17 ± 0.04	> 100	2.2 ± 0.3	45 ± 11	0.12 ± 0.05	> 50	1.75 ± 0.14	6 ± 1.67
DMSO tolerance	10%				10%			
Z factor	> 0.5				> 0.5			
S/N ratio	~8.4				~15			

**Figure 5.** Representatives of label-free screening of A431 on Epic[®]. (A) Fura II based fluorescence kinetic imaging results on A431 cells, upon the addition of correspondent small molecule compounds. (B) Epic[®] label-free detection on A431 cells, upon the addition of correspondent small molecule compounds.

phosphorylation pattern of GPCRs, in which the sites and amount of phosphorylation by a variety of kinases (i.e., GRKs, PKA, tyrosine kinase receptor) dictate the

**Figure 6.** Representative results from the label-free cell-based viral detection. (A) Epic[®] label-free cell-based detection of influenza virus, on A549 cells (human alveolar basal epithelial cells). (B) Neuraminidase activity validation of the Epic[®] label-free cell-based detection of influenza.

downstream pathways (i.e., desensitization and/or arrestin recruitment) (24–26). Interrogation of GPCR phosphorylation on the label-free Epic[®] platform would be most informative with a panel of known specific kinase inhibitors, in combination with kinetic responses from multiple additions, to assess the desensitization and internalization processes. It is worthy to point out that a sophisticated pathway analysis might be needed for the complicated phosphorylation network involving

GPCRs to deconvolve the Epic[®] dynamic mass redistribution (DMR) responses.

Another application is to apply the Epic[®] high-throughput label-free assay to the detection and antiviral drug development. Without further emphasis on the importance of anti-viral drug discovery for emerging threatening epidemics (27), the challenge is still to develop antiviral therapy for the newly emerged virus strain with limited prior knowledge. In this case, the label-free system would likely be the only alternative, since any blind labeling technique without prior knowledge is likely to be unspecific, and thereby compromise its relevance to the real-world situation. Preliminary representative results from the label-free cell-based viral detection are provided in Figure 6. With human basal epithelial cell A549, an influenza viral infection is induced by addition of influenza virus (MOI = 3). The viral infection does induce the Epic[®] signal, without interference from drug alone or medium alone. The addition of drug resulted in 30% decrease of the signal, which is well correlated/validated with the established viral infection detection method of neuraminidase activity detection (28).

In summary, here we present the biochemical interrogation of phosphor-specific interactions of the 14-3-3 protein and its substrates with a high-throughput label-free optical biosensor system, the Epic[®] system. It has shown the capability not only for high-throughput characterization of binding rank and affinity but also for the exploration of potential interacting kinases for the substrates. A perspective of biochemical applications for diagnostics and biomarker discovery, as well as cell-based applications for endogenous receptors and viral infection characterization, are provided as well.

Acknowledgments

We thank members of the Li laboratory for valuable comments on this manuscript. This work is supported by a grant from the National Institutes of Health (to M.L. U54 MH084691, RO1 GM078579), and supported in part by Corning Inc.

Declaration of interest: The authors report no conflicts of interest.

References

- Cooper MA. Optical biosensors: Where next and how soon? *Drug Discov Today* 2006; 11: 1061–7.
- Qavi A, Washburn A, Byeon J-Y, Bailey R. Label-free technologies for quantitative multiparameter biological analysis. *Analyt Bioanal Chem Online*.
- Akiko Saito, Akiko Saito, Kayoko Kawai, Hiroshi Takayama, Tatsuhiko Sudo, Hiroyuki Osada. Improvement of photoaffinity SPR imaging platform and determination of the binding site of p62/SQSTM1 to p38 MAP kinase. *Chemistry-An Asian Journal* 2008; 3: 1607–12.
- Landry JP, Gray J, O'Toole MK, Zhu XD. Incidence-angle dependence of optical reflectivity difference from an ultrathin film on solid surface. *Opt Lett* 2006; 31: 531–3.
- Fang Y, Ferrie AM, Fontaine NH, Mauro J, Balakrishnan J. Resonant waveguide grating biosensor for living cell sensing. *Biophys J* 2006; 91: 1925–40.
- Wu M, Coblitz B, Shikano S, Long S, Spieker M, Frutos AG, Mukhopadhyay S, Li M. Phospho-specific recognition by 14-3-3 proteins and antibodies monitored by a high throughput label-free optical biosensor. *FEBS Lett* 2006; 580: 5681–9.
- Pawson T, Scott JD. Protein phosphorylation in signaling—50 years and counting. *Trends Biochem Sci* 2005; 30: 286–90.
- Yaffe MB. How do 14-3-3 proteins work? Gatekeeper phosphorylation and the molecular anvil hypothesis. *FEBS Lett* 2002; 513: 53–7.
- Shikano S, Coblitz B, Wu M, Li M. 14-3-3 proteins: Regulation of endoplasmic reticulum localization and surface expression of membrane proteins. *Trends Cell Biol* 2006; 16: 370–5.
- Coblitz B, Wu M, Shikano S, Li M. C-terminal binding: An expanded repertoire and function of 14-3-3 proteins. *FEBS Lett* 2006; 580: 1531–1535.
- Wu M, Coblitz B, Shikano S, Long S, Cockrell LM, Fu H, Li M. SWTY—A general peptide probe for homogeneous solution binding assay of 14-3-3 proteins. *Anal Biochem* 2006; 349: 186–96.
- Park Y-W, et al. Homogeneous proximity tyrosine kinase assays: Scintillation proximity assay versus homogeneous time-resolved fluorescence. *Anal Biochem* 1999; 269: 94–104.
- De SK, et al. Design, synthesis, and structure-activity relationship of substrate competitive, selective, and in vivo active triazole and thiaziazole inhibitors of the c-Jun N-terminal kinase. *J Med Chem* 2009; 52: 1943–52.
- Vedvik KL, Eliason HC, Hoffman RL, Gibson JR, Kupcho KR, Somberg RL, Vogel KW. Overcoming compound interference in fluorescence polarization-based kinase assays using far-red tracers. *ASSAY Drug Dev Technol* 2004; 2: 193–203.
- Sun YS, Landry JP, Fei YY, Zhu XD, Luo JT, Wang XB, Lam KS. Effect of fluorescently labeling protein probes on kinetics of protein-ligand reactions. *Langmuir* 2008; 24: 13399–405.
- Tiefenthaler K, Lukosz W. Sensitivity of grating couplers as integrated-optical chemical sensors. *J Opt Soc Am B* 1989; 6: 209–20.
- Wiki M, Dübendorfer J, Kunz RE. Spectral beam sampling and control by a planar optical transducer. *Sensors Actuators A: Physical* 1998; 67: 120–4.
- Huang X. Fluorescence polarization competition assay: The range of resolvable inhibitor potency is limited by the affinity of the fluorescent ligand. *J Biomol Screen* 2003; 8: 34–8.
- Jian-Guo Dai KM. Constitutively and autonomously active protein kinase C associated with 14-3-3 in the rodent brain. *J Neurochem* 2003; 84: 23–34.
- Zhang L, Wang H, Liu D, Liddington R, Fu H. Raf-1 kinase and coenzyme S interact with 14-3-3zeta through a common site involving lysine 49. *J Biol Chem* 1997; 272: 13717–24.
- Wood NT, Meek DW, MacKintosh C. 14-3-3 binding to p14ARF phosphorylated Ser166 and Ser186 of human Mdm2—Potential interplay with the PKB/Akt pathway and p14ARF. *FEBS Lett* 2009; 583: 615–20.
- Lawlor K, Nazarian A, Lacomis L, Tempst P, Villanueva J. Pathway-based biomarker search by high-throughput proteomics profiling of secretomes. *J Proteome Res* 2009; 8: 1489–503.
- Kumon RE, Aehle M, Sabens D, Parikh P, Han YW, Kourennyi D, Deng CX. Spatiotemporal effects of sonoporation measured

- by real-time calcium imaging. *Ultrasound Med Biol* 2009; 35: 494-506.
24. Tobin AB, Butcher AJ, Kong KC. Location, location, location & site-specific GPCR phosphorylation offers a mechanism for cell-type-specific signalling. *Trends in Pharmacological Sciences* 2008; 29: 413-20.
 25. Jurado-Pueyo M, Campos PM, Mayor F, Murga C. GRK2-dependent desensitization downstream of G proteins. *J Recept Signal Transd* 2008; 28: 59-70.
 26. van Der Lee MMC, Bras M, van Koppen CJ, Zaman GJR. β -Arrestin recruitment assay for the identification of agonists of the sphingosine 1-phosphate receptor EDG1. *J Biomol Screen* 2008; 13: 986-98.
 27. Wainberg MA. Perspectives on antiviral drug development. *Antivir Res* 2009; 81: 1-5.
 28. Eichelberger M, Hassantoufighi A, Wu M, Li M. Neuraminidase activity provides a practical read-out for a high throughput influenza antiviral screening assay. *Virology* 2008; 5: 109.